

Study of $\pi\pi$ production in two-photon collisions at Belle

S. Uehara¹⁾ (for the Belle Collaboration)

(IPNS-KEK, Institute of Particle and Nuclear Studies,
High Energy Accelerator Research Organization, Tsukuba, Japan)

Abstract We have measured the cross section for $\pi^+\pi^-$ production in two-photon collisions using a data sample with an integrated luminosity of 85.9 fb^{-1} collected with the Belle detector. The $f_0(980)$ resonance is observed as a peak in the energy spectrum of the cross section. We also report preliminary results for $\gamma\gamma \rightarrow \pi^0\pi^0$ with two-photon center-of-mass energies ranging from 0.6 to 4.0 GeV, based on a 95 fb^{-1} data sample. We find at least four resonant structures including a peak from $f_0(980)$. In addition, there is evidence for χ_{c0} production. We also make a preliminary discussion of the angular dependence and cross section ratio of $\gamma\gamma \rightarrow \pi^+\pi^-$ and $\gamma\gamma \rightarrow \pi^0\pi^0$.

Key words two-photon collisions, pion, cross section, resonances, charmonia

PACS 13.20.Gd, 13.60.Le, 13.66.Bc, 14.40.Cs, 14.40.Gx

1 Introduction

Measurements of exclusive hadronic final states in two-photon collisions provide valuable information about the physics of light and heavy-quark resonance production, perturbative and non-perturbative QCD and hadron-production mechanism. In this report, we show results from measurements of pion-pair production in two-photon processes for both charged and neutral pion pairs^[1]. Although the physics motivation is essentially the same for the charged and neutral pion processes, the two processes are physically independent.

For the low energy region (the two-photon center-of-mass energy range, $W < 1.0 \text{ GeV}$), it is expected that different electric charges of the mesons play an essential role in the difference of the cross sections between the $\pi^+\pi^-$ and $\pi^0\pi^0$ processes. The predictions are not easy because of non-perturbative effects. For the intermediate energy region, the formation of meson resonances decaying to $\pi\pi$ is the dominant contribution. We can restrict $I^G J^{PC}$ states of the $q\bar{q}$ mesons produced in the processes to be $0^+(\text{even})^{++}$, that is, $f_{J=\text{even}}$. Although isospin invariance provides the ratio of the branching fractions, $\mathcal{B}(f_J \rightarrow \pi^0\pi^0)/\mathcal{B}(f_J \rightarrow \pi^+\pi^-) = 1/2$, interferences of

resonances with continuum components which cannot be precisely calculated distort the ratio even near the resonant peak energies.

For high energies, we invoke a quark model. In the leading order calculations^[2, 3], the $\pi^0\pi^0$ cross section is predicted to be much smaller than that of $\pi^+\pi^-$, around 0.03—0.06, in the cross section ratio of $\pi^0\pi^0$ to $\pi^+\pi^-$. However, higher-order or non-perturbative QCD effects can modify the ratio. For example, the handbag model which considers soft hadron exchange predicts the same amplitude for the two processes, and this ratio becomes 0.5^[4]. Analyses of energy and angular distributions of the cross sections are also essential to test the validity of QCD models.

We report results of the measurement of the differential cross section, $d\sigma/d|\cos\theta^*|$, for $\gamma\gamma \rightarrow \pi^+\pi^-$ ^[5] and preliminary results for $\gamma\gamma \rightarrow \pi^0\pi^0$ for a wide two-photon center-of-mass (c.m.) energy range from 0.6 to 4.0 GeV, and a c.m. angular range, $|\cos\theta^*| < 0.8$ ^[6]. For the latter measurement, our data sample has several hundred times larger statistics than in previous experiments^[7, 8].

2 Accelerator and detector

We use data collected with the Belle detector^[9] at the KEKB asymmetric-energy e^+e^- collider^[10]. The

Received 17 January 2008

1) E-mail: uehara@post.kek.jp

energy of the accelerator was set at 10.58 GeV for the greater part of the data and at 10.30 — 10.52 GeV for a small fraction of the data. The analysis is made in the “zero-tag” mode, where neither the recoil electron nor positron is detected. We restrict the virtuality of the incident photons to be small by imposing a requirement of a strict transverse-momentum balance along the beam axis of the final-state hadronic system.

3 Measurement of $\gamma\gamma \rightarrow \pi^+\pi^-$

We have recently published our measurement of charged-pion pair production for low energies^[5]. Separately, we have a measurement of the same process for the higher energy region 2.4 — 4.1 GeV^[11].

The $f_0(980)$ is a mysterious meson whose true nature is not yet known; there is no definite place for this particle in the $q\bar{q}$ meson assignment table. It might be an exotic state, or might be explained by some theoretical models. The two-photon decay width which directly provides information about its contents is a crucial key. In our measurement we found that the $f_0(980)$ emerges as a small peak in the spectrum of this process, as shown in Fig. 1, which so far has been concealed by the large tail of the $f_2(1270)$ resonance and the continuum component.

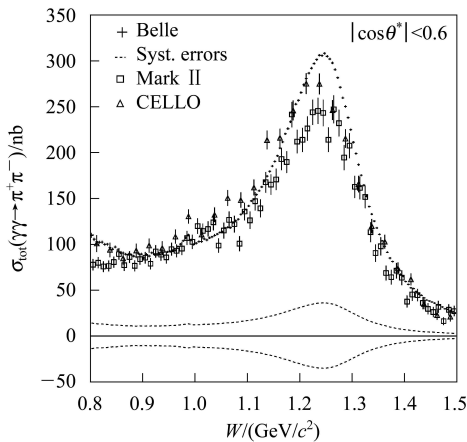


Fig. 1. The cross section of $\gamma\gamma \rightarrow \pi^+\pi^-$ for $|\cos\theta^*| < 0.6$. The Belle data are represented by small crosses. The error bars are statistical only. Dashed lines are upper and lower systematic uncertainties for the Belle data.

Figure 2 shows an enlarged view near the $f_0(980)$ region. The peak is significant with large statistics. We fit the resonance line shape and obtain the resonance parameters as

$$M = 985.6_{-1.5}^{+1.2}(\text{stat.})_{-1.6}^{+1.1}(\text{sys.}) \text{ MeV}/c^2,$$

$$\Gamma_{\pi^+\pi^-} = 34.2_{-11.8}^{+13.9} \text{ }_{-2.5}^{+8.8} \text{ MeV}$$

and $\Gamma_{\gamma\gamma} = 205_{-83}^{+95} \text{ }_{-117}^{+147} \text{ keV}$, for the mass and the $\pi^+\pi^-$ and $\gamma\gamma$ partial decay widths of the $f_0(980)$,

respectively. Although the two-photon decay width is significantly smaller than for ordinary $u\bar{u}/d\bar{d}$ resonances, we cannot still conclude whether it is really an exotic state.

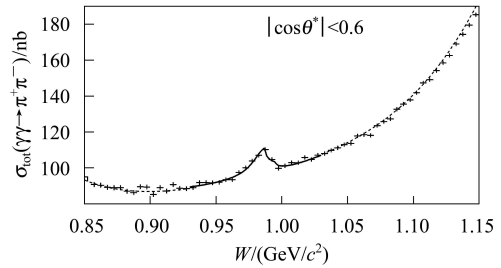


Fig. 2. The cross section and the fitted curve near the $f_0(980)$.

We do not find any peak structure near the η' mass ($\sim 0.958 \text{ GeV}/c^2$). We obtain a new upper limit of the branching fraction of $\eta' \rightarrow \pi^+\pi^-$, which violates P and CP . The upper limit at 90% confidence level, $\mathcal{B}(\eta' \rightarrow \pi^+\pi^-) < 2.8 \times 10^{-3}$ ($< 3.3 \times 10^{-4}$), is obtained assuming presence (absence) of the interference effect with the continuum $\gamma\gamma \rightarrow \pi^+\pi^-$ component. These limits are much stricter than the previous one of 2%^[12].

4 Measurement of $\gamma\gamma \rightarrow \pi^0\pi^0$ ^[6]

4.1 Trigger and event selection

The neutral pion process has only photons in the final state. We use only events triggered by activity in the electromagnetic calorimeter, ECL. We have two kinds of ECL triggers. The high-threshold total-energy trigger accepts events with the threshold around 1.15 GeV. The other trigger requires four or more energy clusters with a threshold around 110 MeV for each. We determine the trigger efficiency for signal events using a trigger simulation program.

We collect events with multiple photons without any reconstructed tracks. Just two reconstructed neutral pions are required. We apply a transverse-momentum (p_t) balance cut for the two-pion system in the e^+e^- c.m. frame, $|\Sigma p_t^*| < 0.05 \text{ GeV}/c$.

4.2 Candidate events and background subtractions

After the event selection, we find about 1.26×10^6 candidates for $\gamma\gamma \rightarrow \pi^0\pi^0$. The invariant-mass distributions of these events in specified angular ranges are shown in Fig. 3. We find some resonant structures as well as hints for χ_{cJ} ($J=0, 2$) charmonia.

The curve drawn in Fig. 3(a) is a background estimated from the p_t balance distribution of the two-pion system; we find a rather big contamination of

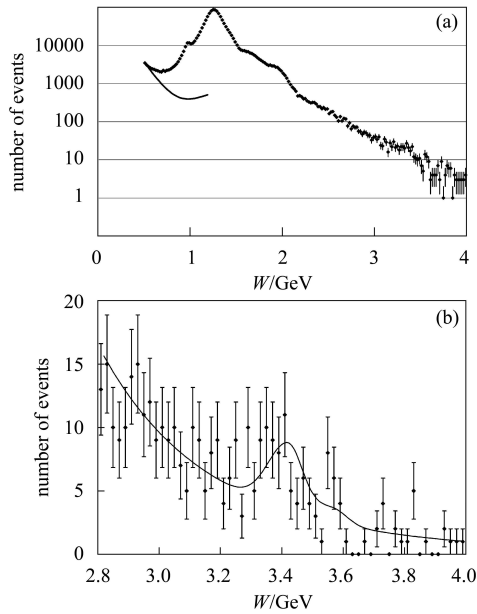


Fig. 3. The W distributions of the candidate events. (a) $|\cos\theta^*| < 0.8$. The curve shows estimated p_t -unbalanced backgrounds. (b) $|\cos\theta^*| < 0.4$, near the charmonium region. The curve is the fit taking the χ_{cJ} charmonia into account.

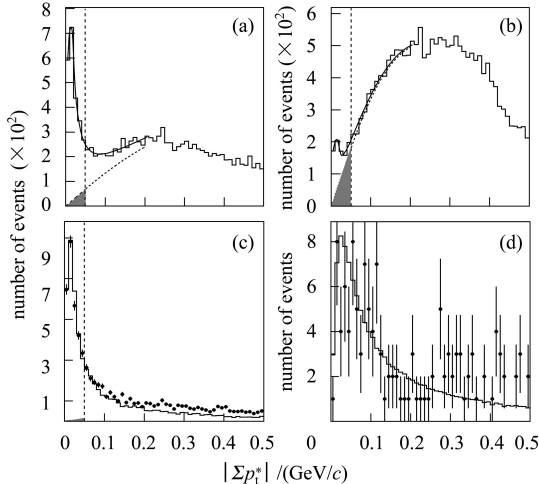


Fig. 4. The distribution of imbalance in p_t for candidate events. (a) In the bin centered at $W = 0.90$ GeV and $|\cos\theta^*| = 0.05$ (The bin width is 0.04 GeV and 0.1 in the W and $|\cos\theta^*|$ directions, respectively, in (a)–(c).), the experimental distribution (histogram) is fitted with the sum of signal and background components (curves). The grey region shows the estimated background contamination in the signal region. (b) $W = 0.66$ GeV, same as in (a) for the others. (c) In the bin of $W = 1.18$ GeV, $|\cos\theta^*| = 0.65$, the experimental distribution (dots with error bars) is compared with the signal MC (histogram). The grey region shows the estimated background contaminating the signal region obtained from the fit. (d) For $3.6 < W < 4.0$ GeV and $|\cos\theta^*| < 0.4$, the experimental distribution (dots with error bars) is compared with the signal MC (histogram).

the p_t -unbalanced component for $W < 0.9$ GeV, as found in Figs. 4(a,b). We can separate them using fits including the signal and background components. For energies above 1.1 GeV, the background is much smaller than the signal, and any significant contributions from the background cannot be identified in the distributions (Figs. 4(c,d)).

The invariant-mass resolution is estimated using signal Monte Carlo (MC) events and the experimental p_t balance distributions. The invariant-mass resolution is determined to be about 1.6%, almost independent of the energy. We confirm the energy scale and resolution using the $\eta' \rightarrow \gamma\gamma$ events produced in two-photon collisions. By modeling this smearing effect of the resolution, we applied an unfolding procedure to obtain the corrected invariant-mass distribution between 0.9 and 2.4 GeV for each angular bin with a width $\Delta|\cos\theta^*| = 0.05$.

4.3 Derivation of cross sections

The acceptance, i.e. the efficiency of the selection not including that of the trigger, is determined using the signal MC events for each bin. It has a rather large angular dependence due to a geometrical restriction of the detector and is smaller for small angles. We obtain preliminary cross sections as a function of W . We first derive $d\sigma/d|\cos\theta^*|$ in 16 angular bins in $|\cos\theta^*| < 0.8$ and then integrate them over the angle. The result is shown in Fig. 5. Data points in

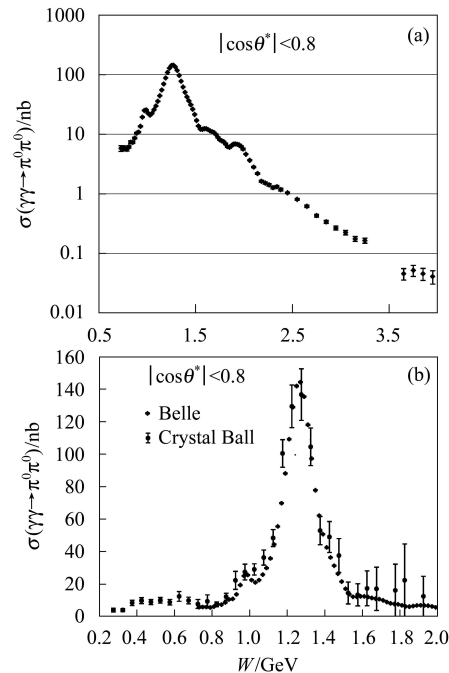


Fig. 5. The cross section of $\gamma\gamma \rightarrow \pi^0\pi^0$ for $|\cos\theta^*| < 0.8$. In (b) a part of the present results is compared with the Crystal-Ball measurements^[8].

the energy region where the contribution from χ_{cJ} charmonia is dominant are removed, because we cannot separate the components from χ_{c0} , χ_{c2} and the continuum in a model-independent way, due to the finite mass resolution and insufficient statistics.

We estimate the systematic errors for the integrated cross sections. We assign a 4% error to the uncertainty of the total energy trigger. For low energies, the four-cluster energy has a larger uncertainty (up to 30%) at $W = 0.61$ GeV. Other major error sources are π^0 reconstruction efficiency (6% for two pions), background subtraction (sizeable only for $W < 0.8$ GeV), luminosity function (4%–5%). The total systematic error is about 9% for $1.0 \text{ GeV} < W < 2.4$ GeV. For lower energies, the error gets much bigger, e.g. about 27% at $W = 0.73$ GeV. Above 2.4 GeV, the error is not so large, 10%–11%.

4.4 Discussion

Our results are consistent with the previous measurement by Crystal Ball at DORIS II^[8], as seen in Fig. 5(b). Our data has several hundred times larger signal statistics than in the Crystal Ball measurement.

We find prominent resonant structures near 0.98 GeV, 1.27 GeV, 1.65 GeV and 1.95 GeV. The first two are from $f_0(980)$ and $f_2(1270)$, respectively, which are also observed in the $\gamma\gamma \rightarrow \pi^+\pi^-$ process^[5]. The latter two cannot readily be assigned to any well-known states. In addition, we find hints of other possible resonant structures at around 1.45 GeV and near the masses of the two charmonia χ_{c0} and χ_{c2} .

We fit the distribution of the yield for the range $2.8 \text{ GeV} < W < 4.0$ GeV and $|\cos\theta^*| < 0.4$ with a function including the contributions from the χ_{c0} and χ_{c2} and a smooth contribution from the continuum with a binned maximum-likelihood method. The fit is shown in Fig. 3(b). We take into account effects of the finite

invariant-mass resolution in the resonance function. The mass and width of the charmonia are fixed to the world averages^[12]. We obtain the yields 35.3 ± 9.2 events and 8.2 ± 6.4 events for χ_{c0} and χ_{c2} , respectively. From the yields we extract the products of the two-photon decay width and the branching function, $\Gamma_{\gamma\gamma}(\chi_{cJ})\mathcal{B}(\chi_{cJ} \rightarrow \pi^0\pi^0) = 8.4 \pm 2.2 \pm 0.8$ eV and $0.29 \pm 0.23 \pm 0.03$ eV, for χ_{c0} and χ_{c2} , respectively. The latter corresponds to an upper limit with 90% C.L., $\Gamma_{\gamma\gamma}(\chi_{c2})\mathcal{B}(\chi_{c2} \rightarrow \pi^0\pi^0) < 0.75$ eV. The central values are in good agreement with the corresponding world averages^[12] which are dominantly relying on the Belle measurements of the charged pion pair decays^[11], taking isospin invariance into account.

The general trend of the angular dependence of the differential cross section is as follows: it has a maximum at $|\cos\theta^*| = 0$ for $W < 2.1$ GeV. For $W > 1.9$ GeV, however, the angular dependence shows a rise toward the forward angles. As W increases, the point at which the differential cross section in the c.m. angle begins to rise moves toward forward angles, and the rise steepens. Angular dependence of the differential cross section at five energy points is shown in Fig. 6.

We show the cross section ratio between $\gamma\gamma \rightarrow \pi^0\pi^0$ and $\gamma\gamma \rightarrow \pi^+\pi^-$ ^[11] for $|\cos\theta^*| < 0.6$ and $2.4 \text{ GeV} < W < 4.0$ GeV, in Fig. 7. In the figure, the error bars are statistical only, and each cross section measurement has typically a 10% systematic error. The data points of $\gamma\gamma \rightarrow \pi^+\pi^-$ above the charmonium masses have larger systematic error, $\sim 25\%$.

The ratio seems to have no big energy dependence for $W > 2.7$ GeV and has a value around 0.3–0.4. This ratio is larger than the prediction from the lowest-order QCD calculation^[2, 3]. We, however, need more detailed investigations of the W and angular dependences in comparison with the predictions of the QCD models to test the expected asymptotic nature.

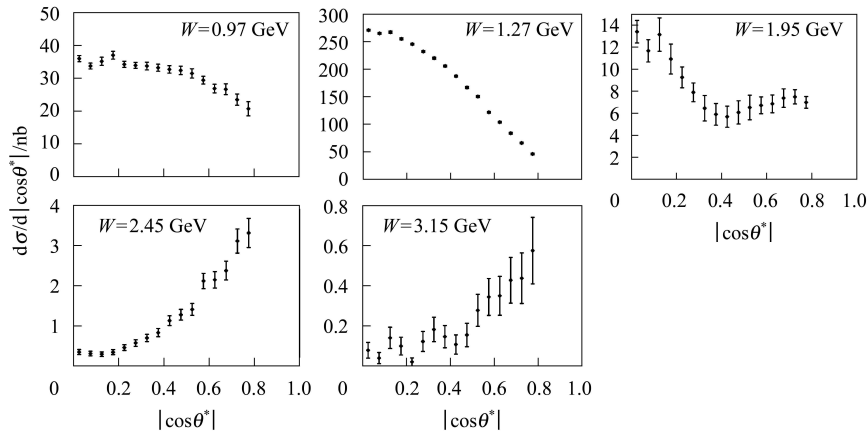


Fig. 6. The differential cross sections at five selected W points.

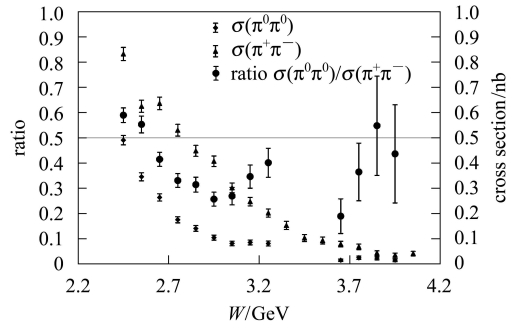


Fig. 7. Ratio of the cross section of $\gamma\gamma \rightarrow \pi^0\pi^0$ to that of $\gamma\gamma \rightarrow \pi^+\pi^-$ for $|\cos\theta^*| < 0.6$ (closed circles). The diamonds and the triangles are the cross sections of the two processes. The error bars are statistical only.

5 Summary

We have measured the cross section of the process $\gamma\gamma \rightarrow \pi^+\pi^-$ for the c.m. energy region between 0.8 and 1.5 GeV. We observe a significant peak from the $f_0(980)$, and its resonance parameters are obtained^[5].

We have measured the preliminary cross section of the process $\gamma\gamma \rightarrow \pi^0\pi^0$ for the c.m. energy and angular regions, $0.60 \text{ GeV} < W < 4.0 \text{ GeV}$ and $|\cos\theta^*| < 0.8$ ^[6]. We observe some resonant structure, including the $f_0(980)$. We find that the angular dependence changes drastically at around $W = 2.0 \text{ GeV}$. The ratio of the cross sections of $\gamma\gamma \rightarrow \pi^0\pi^0$ and $\gamma\gamma \rightarrow \pi^+\pi^-$ in the 3 GeV region is obtained.

References

- 1 Uehara S. Proceedings of Photon2007, International Conference on the Structure and Interactions of the Photon including the 17th International Workshop on Photon-Photon Collisions and the International Workshop on High Energy Photon Linear Colliders. Paris, 9-13 July 2007, to be published in Nucl. Phys. B (Proc. Suppl.).
- 2 Brodsky S J, Lepage G P. Phys. Rev. D, 1981, **24**: 1808
- 3 Benayoun M, Chernyak V L. Nucl. Phys. B, 1990, **329**: 209; Chernyak V L. Phys. Lett. B, 2006, **640**: 246
- 4 Diehl M, Kroll P, Vogt C. Phys. Lett. B, 2002, **532**: 99
- 5 Belle Collaboration, Mori T et al. J. Phys. Soc. Jpn., 2007, **76**: 074102; Belle Collaboration, Mori T et al. Phys. Rev. D, 2007, **75**: 051101(R)
- 6 Belle Collaboration, Abe K et al. BELLE-CONF-0768, arXiv.0711.1926, 2007
- 7 JADE Collaboration, Oest T et al. Zeit. Phys. C, 1990, **47**: 343
- 8 Crystal Ball Collaboration, Marsiske H et al. Phys. Rev. D, 1990, **41**: 3324
- 9 Belle Collaboration, Abashian A et al. Nucl. Instrum. Methods A, 2002, **479**: 117
- 10 Kurokawa S, Kikutani E. Nucl. Instrum. Methods A, 2003, **499**: 1 and other papers included in this volume.
- 11 Belle Collaboration, Nakazawa H et al. Phys. Lett. B, 2005, **615**: 39
- 12 Particle Data Group, Yao W-M et al. J. Phys. G, 2006, **33**: 1